Catalysis Letters Vol. 105, Nos. 3–4, December 2005 (© 2005)
DOI: 10.1007/s10562-005-8683-8

Silica nanoboxes as new nano-structured materials: their secondary synthesis from alumina-rich zeolites

L. Lu, R. Le Van Mao*, N. Al-Yassir, A. Muntasar, and N. T. Vu

Industrial Catalysis Laboratory and Laboratories for Advanced Inorganic Materials, Department of Chemistry and Biochemistry, Concordia University, 7141 Sherbrooke West, SP 275-09, Montreal (Quebec) H4B 1R6, Canada

Received 7 June 2005; accepted 23 August 2005

Novel *silica nanoboxes* were prepared by controlled dealumination of Na-X and Ca-A type zeolites using ammonium hexafluorosilicate (AHFS). The silica-richer the parent zeolite, the smaller the average pore size produced and the narrower the pore size distribution obtained. This was due to the specific reactivity of the extracting agent with the zeolite framework aluminum atoms. High temperature calcination of the dealuminated X-zeolite (ammonium form) resulted in mesoporous materials exhibiting an ink-bottle shape, a quite high surface area (330 m^2/g, no micropores), an average pore diameter of 4.5 nm with a quite narrow pore size distribution (±1.0 nm) and finally, a pore opening diameter of 3.9 nm. The latter was determined by using the nitrogen sorption isotherms (BET technique) and related pore volume data. The sorption behavior also suggested the *interconnecting character* of the newly created nanoboxes. The *periodicity* of these nanoboxes throughout the mesoporous material was clearly shown by X-ray powder diffraction at very small angles. These materials, herein called monomodal nanoboxes because of the absence of micropores in the structure, were also *thermally stable*. Incorporation of orthosilicate into the obtained silica nanoboxes, in accordance with the recently developed technique for pore size engineering in zeolites, led to materials with *smaller pore openings* but having almost the same textural properties. Solid superacidic materials were prepared by incorporating a liquid superacid (triflic acid or trifluoromethanesulfonic acid) into the silica nanoboxes using the wet impregnation technique. The maximum triflic acid loading which did not significantly affect the mesoporous framework of the materials was 24 wt%. As a reference, the maximum loading of less acidic sulfuric acid was slightly lower. All this showed the *high chemical stability* of the silica nanoboxes for supporting very acidic species. Temperature-programmed desorption using a combined DTA/TGA system allowed the identification of the bound phases and some liquid phase of the loaded triflic acid.

KEY WORDS: silica nanoboxes from zeolites; pore characteristics; thermal/chemical stability; surface acidity.

1. Introduction

Zeolites are very interesting materials for catalysis and separation technology owing to their microporous network. However, larger substrate molecules require mesoporous materials, also called nanomaterials or nanostructured materials, which exhibit a structure based on a periodic arrangement of mesopores such as the synthetic MCM-41 [1,2]. Unfortunately, these materials are known to be quite thermally and chemically unstable [3]. In the past, we have shown that mesoporous materials can be obtained from Al-rich zeolites by controlled dealumination using ammonium hexafluorosilicate (AHFS) as Al removing agent [4–7]. This is in contrast with more aggressive Al removing media such as mineral acids which usually lead to severe structural collapses and thus not very useful mesoporous materials because the latter are subject to numerous pore occlusions [8] or a lack of direct connection with the external surface of the treated zeolite particle [9]. It is also said that AHFS can substitute the zeolite Al sites by its own Si atoms [10].

* To whom correspondence should be addressed.
E-mail: lvmao@vax2.concordia.ca

In our previous work [6,7], it was shown however that the pore enlargement using the AHFS method could occur without significant pore occlusion. In addition, A and X type zeolites led to different mesoporous materials: in particular, larger mesopores were obtained with Al-richer zeolites [6,7].

Therefore, this work aimed at:

(a) Identifying the shape of the nanosized cavities of the obtained mesoporous materials, their periodicity and their interconnecting character;
(b) Studying their thermal stability;
(c) Evaluating the possibility of modifying their pore size by using the technique of pore size engineering which was successfully applied to the ZSM-5 zeolite [11];
(d) Investigating their chemical stability by loading strong liquid acids such as sulfuric acid and superacidic species such as triflic acid.

2. Experimental

2.1. Controlled dealumination of NaX and CaA zeolites

The controlled dealumination of the NaX and CaA was carried out with a solution of ammonium

1011-372X/05/1200–0139/0

hexafluorosilicate (AHFS) in a manner similar to that reported in Refs. [4–7,12]. The basic procedure was as follows: 2.7 g of NaX or 5.0 g of CaA zeolite (all in powder form) were placed into a Teflon beaker containing 200 cm^3 of 0.8 mol dm^{-3} ammonium acetate solution (pH of ca. 7.0). Then 20 cm^3 of a freshly prepared 0.5 mol dm^{-3} ammonium hexafluorosilicate (Aldrich) aqueous solution were added, under vigorous stirring, to the suspension using an injection syringe on an infusion pump. The rate of AHFS addition was kept at 0.81 and 1.7 cm^3 min^{-1} for NaX and CaA, respectively. Then the medium was heated at 80°C in the water bath after the AHFS addition was completed. The mild stirring was continued for 1 h. The solid was then separated by filtration and washed on the filter five times, each time with ca. 300 cm^3 of distilled water. The product was dried in an oven at 110°C overnight in the air and then activated at 250°C for 4 h. The resulting solids were named (m) Na-deal X and (m) deal CaA, respectively, m stands for monomodal materials. In fact, as we will see in the following, this dealumination method resulted in totally mesoporous solids, i.e., there was no or very little microporosity, with quite narrow pore size distribution for the (m) Na-deal X.

However, bimodal materials which contained a large portion of mesopores and some micropores (remnants of the parent zeolite structure), were obtained using milder dealumination conditions as follows. 10.0 g of NaX zeolite (in powder form) were placed into a Teflon beaker containing 200 cm^3 of 0.8 mol dm^{-3} ammonium acetate solution (pH of ca. 7.0). Then 25 cm^3 of a freshly prepared 0.5 mol dm^{-3} ammonium hexafluorosilicate (Aldrich) aqueous solution were added, at room temperature and under vigorous stirring, to the suspension using an injection syringe on an infusion pump. The rate of AHFS addition was kept at 0.90 cm^3 min^{-1}. The slurry was then left at room temperature, always under vigorous, for 2 h. The solid was then separated by filtration and washed on the filter three times, each time with ca. 200 cm^3 of hot water. The product was dried in an oven at 110°C overnight in the air and then activated at 250°C for 4 h. The resulting material was named (b) Na-deal X.

2.2. Thermal treatment of the deal X (Na and NH_4 forms) and deal CaA

In order to ion-exchange Na^+ with NH_4^+, the (m) Na-deal X sample (or (b) Na-deal X) was treated with an aqueous solution of NH_4Cl (5 wt%) in a Teflon beaker, using 10 cm^3 of NH_4Cl solution for 1 g of zeolite, and heated at 80°C under mild stirring for 2 h. This procedure was repeated twice for a total of 6 h. After each treatment, the used solution was decanted and a fresh solution of NH_4Cl was added. The resulting material was separated by vacuum filtration and washed on the filter with water.

The product was dried in an oven at 110°C overnight in the air and then activated at 250°C for 4 h. The resulting solid was called herein (m) NH_4-deal X (or (b) NH_4-dealX). The acid form ((m) H-deal X,TPC) was obtained by activating the (m) NH_4-deal X sample using a stepwise heating procedure (TPC or temperature-programmed calcination), i.e., 300°C for 3 h, then gradual heating to 600°C at a rate of 50°C per hour, finally heating at 600°C for 18 h. Calcined (m) Na-deal X and deal CaA samples were obtained using the same heating procedure.

Another calcination procedure was also used (direct heating (DH)) which consisted of heating the solid material at 300°C for 3 h, then rapidly increasing the temperature to 600°C and finally keeping at that temperature for 3 h.

2.3. Modification of the pore opening of the (m) H-deal X and increasing its wall thickness

Ion exchange of sodium orthosilicate (Na_4SiO_4) with H^+ was performed on Amberlyst 15 ion-exchange resin (acid form). 5.2 g of the acidic resin was packed in a glass column and wetted with distillated water, then 5 cm^3 of aqueous solution of orthosilicate (6 wt%, kept in Teflon bottle) were passed through the resin column, using distillated water as elutant. The volume of the collected brownish liquid was ca. 60 cm^3 and was assumed to contain the orthosilicic acid (H_4SiO_4). From 5 to 30 g of the obtained liquid (depending on the amount of orthosilisic acid needed) were then concentrated to a volume of 1–2 cm^3 in a rotovap under vacuum and heated at 74°C. (m) H-deal X was then placed in this H_4SiO_4 solution; the evaporation was continued until the solid was completely dried. The resulting solid was further dried in an oven at 110°C overnight in the air and then calcined using the same procedure as described earlier.

2.4. Loading of the triflic acid and the sulfuric acid into the (m) H-deal X

Triflic acid (trifluoromethanesulfonic acid) is one of the strongest acids known, yet it is nonoxidizing. It does not provide fluoride ions, and possesses superior thermal stability and resistance to both oxidation and reduction [13].

Well-defined volumes of aqueous solution of triflic acid (0.0149 g cm^{-3} of water) or sulfuric acid (0.0151 g cm^{-3} of water) were added to 0.2 g of (m) H-deal X sample to achieve 7, 10, and 15 wt% or more of acid loading. The suspension was then placed in the fume hood, at room temperature, to evaporate all the water for more than 5 h. The apparently dried solid was further dried in the oven at 110°C in the air overnight.

2.5. Characterization of the solid materials

Atomic absorption spectroscopy was used for the determination of the chemical composition (Si/Al atom ratio). X-ray powder diffraction patterns were collected on a Siemens D500TT automated diffractometer using Cu(Kα) radiation (λ = 1.5405981 Å), and equipped with a diffracted-beam graphite monochromator, a scintillation detector and solid state counting electronics. The generator voltage and current settings were 45 kV and 40 mA, respectively. In particular, X-ray powder diffraction at small angles [over the angular range of 1–10.2° (2θ) in 0.02° steps and a count time of 1 s/step] was used to show the periodicity of the nanosized cavities in the network of the silica nanoboxes. This was also carried out under highly collimated slit arrangement with the sample (+ holder) and then the holder alone, in order to confirm that it was true diffraction and not an optical artefact due to slits.

The determination of textural properties (BET surface area, nitrogen adsorption/desorption isotherms, pore size distribution using the desorption BJH method [14]) was carried out with a Micromeretics ASAP 2000 Model system. The IUPAC nomenclature [15] is used in this paper, i.e., micropores are pores whose size is below 2 nm whereas mesopores have sizes which range from 2 to 50 nm. The pore size distribution was investigated by plotting the differential pore volume $F = dV/d\log D$ as a function of the pore diameter D (desorption phase, V and D in cm^3 and nm, respectively).

Thermogravimetric (TGA) and differential thermal (DTA) analyses using a PL Thermal Sciences, STA-1500 Model DTA/TGA apparatus might help identify the acidic species incorporated into the material as deposited liquid form and bound-to-the-surface forms [16].

3. Results and Discussion

3.1. Crystallinity and pore characteristics of the new mesoporous materials

Treatment of a zeolite rich in Al such as the CaA and NaX with the AHFS in buffered medium involved the following reaction [10]:

$$Na^+AlO_4^- + (NH_4)_2SiF_6 \rightarrow SiO_4 + (NH_4)_2AlF_5 + NaF$$

The species underlined in the previous equation represented species which were connected to the zeolite framework since it was suggested that AHFS led to the substitution of surface Al sites by the Si species of the AHFS [10].

However, this work showed – also in accordance with the results of refs [4–7] – that:

(a) most of the SiO_4 species formed by this reaction, were not reinserted into the zeolite framework: they were instead removed by the AHFS solution, leading to empty sites on the zeolite surface. This Al removing phenomena, being gradual and homogeneous when the treatment conditions were mild and controlled, resulted in a general pore enlargement.
(b) Some other SiO_4 species remained trapped in the newly formed cavities and might affect the pore characteristics of the mesoporous materials (pore occlusion) when activated at high temperature because these debris were quite mobile [11].

X-ray powder diffraction showed that the original crystallinity of the NaX zeolite almost completely disappeared upon AHFS treatment. However, a new peak at 2θ of around 1.26° (corresponding to a d-spacing of less than 7 nm) was clearly identified (see figure 1 of sample (m) H – deal X, and also the procedure for the elimination of eventual optical artifacts in the section Characterization of the solid materials). This means that the new materials had a framework with a high periodicity in nanosized cavities. This recalls the diffraction pattern of MCM-41 [17] whose all-silica form exhibited a very strong reflection at 3.62 nm and very weak reflections at 2.12, 1.86, and 1.41 nm. However, with the increase in the aluminum content of the material, the main intense peak shifted towards higher d-spacing. In addition, the main peak became broader and less intense, suggesting a poorly crystalline nature of the material. Moreover, the weak reflections became much weaker and were not seen in the case of the MCM-41 with Si/Al close to 2 [17]. This situation was very similar to that of our (m) H-deal X sample.

On the other hand, the sorption isotherms of the AHFS treated zeolites which showed important hysteresis loops – in contrast with those of the parent zeolites – were indicative of almost totally mesoporous materials (figure 2). It is worth mentioning that a hysteresis loop is created by the difference in behavior of adsorption and desorption, resulting in a difference in the shape of sorption isotherms, mainly in the mesopore region. This difference stems from the value of cos θ [18] and also from the shape of the pores if capillary condensation is considered. The equation which is normally used is the Kelvin equation [18,19]. It is also worth noting that the isotherms of adsorption/desorption of the parent zeolites (figure 2a for Na-X zeolite and figure 2c for Ca-A) did not show any hysteresis loop, even in the region of relatively high relative pressure: this suggests that there was no apparent effect of (nitrogen) interparticle uptake or desorption. Since the dealuminated samples ((m) deal-Na-X and deal-CaA) exhibited the same particle sizes as their corresponding parent zeolites, the hysteresis loops reported in figure 2b, d for these dealuminated materials could be correctly abscribed to intracrystalline sorption phenomena.

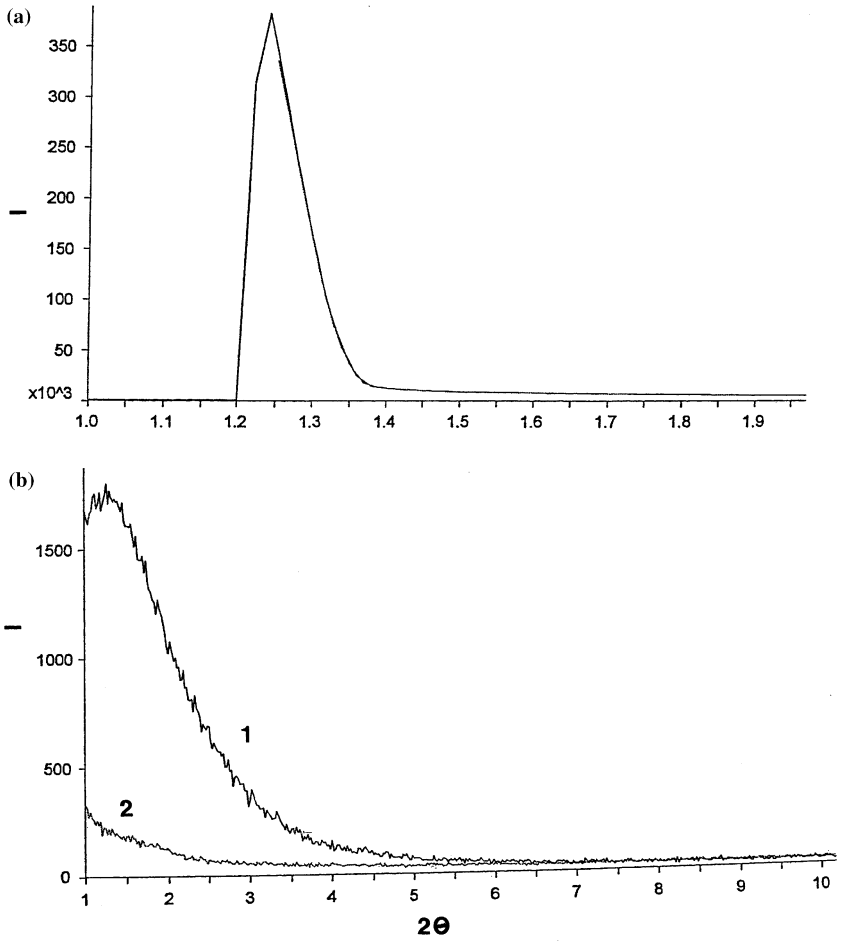

Figure 1. X-ray diffraction at low angle of the (m) H-deal X sample (I = intensity (CPS) versus 2θ. A = diffraction under normal (1°) collimation slit arrangement; B = diffraction under highly collimated slit arrangement (0.1°): 1 = sample, 2 = zero-background holder).

3.1.1. Determination of the pore opening

In the case of our mesoporous materials, since the adsorption isotherms of these materials had all the shape of type IV isotherm and their hysteresis loops were of type E loop, it was assumed that the shape of their pores was that of an ink-bottle (figure 3a) or spheroidal cavity – type II ink-bottle – (figure 3b) [19,20a]. In the mesopore region, the relative pressures for both adsorption and desorption isotherms are relatively high (close to 1) so that $\cos\theta$ can be assumed equal to 1 (high wettingness of the pore walls) [21]. Thus, in that case, the adsorption isotherm is less affected by the shape of the pores than the corresponding desorption branch. This allows us to say that the average value of the pore size determined using the adsorption isotherm is closer to the real value than that determined using the desorption isotherm. In effect, because of the influence of the pore shape, there is always some delay in the desorption process resulting thus in narrower calculated pore size (average), i.e.,

$$D_{\mathrm{av}}^{\mathrm{ads}} > D_{\mathrm{av}}^{\mathrm{des}}$$

(average pore diameters in the adsorption and desorption phases, respectively).

Figure 3a, b show that in the desorption phase, only the volume ABCD for both shapes is effectively desorbed, i.e.,

$$V_{\mathrm{ABCD}} = V_{\mathrm{rl}}$$

(cylinder having a diameter equal to the pore opening).

If there were no significant effect of the shape of the pore, i.e. the pores were perfectly cylindrical with the pore diameter equal to the calculated value of the average pore diameter, the volume would be as follows:

$$V_{\mathrm{A'B'C'D'}} = V_{\mathrm{l}}$$

(cylinder having a diameter equal to the average pore size).

This situation can be assumed as that of the adsorption over the calculated value of the average pore diameter, as mentioned earlier.

It is obvious that the two (ABCD) and (A′B′C′D′) cylinders have the same length l.

In the two figure 3a, b, the following volumes are equal to each other:

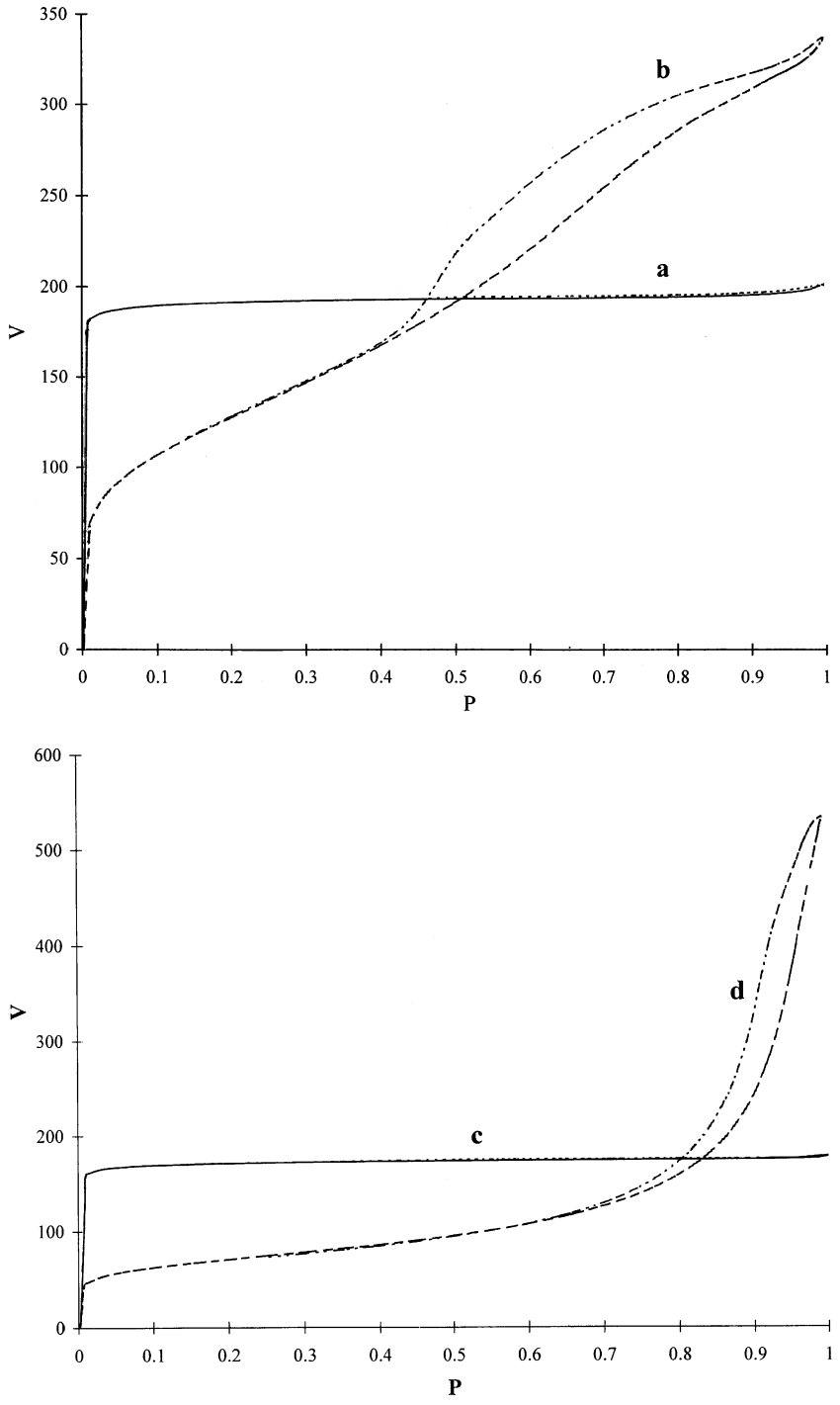

Figure 2. Nitrogen adsorption and desorption isotherms (v = sorbed volume in cm^3 STP g^{-1} versus p = relative pressure P/P_o) of: (a) parent Na-X zeolite; (b) (m) deal-NaX, activated at 250°C; (c) parent Ca-A; (d) deal-CaA activated at 250°C.

$$(ABCC'C''E''E'F'F''D''D'DA)(\text{bottle}) = (A'B'C'E'F'D'A')(\text{cylinder})$$

$$(ABCC'GD'DA)(\text{spheroidal}) = (A'B'C'E'F'D'A')(\text{cylinder})$$

Therefore, V_{rl} and V_l can be experimentally determined using the desorption and adsorption isotherms, respectively. Since the levels CC′C″ DD′D″ and CC′DD′ in both pore configurations correspond to the levels of adsorption or desorption change from the larger pore diameter to the value of average pore size (desorption phase) or *vice-versa* (adsorption phase), knowing the value of the average pore size allows the determination of V_{rl} and V_l using the tables of BET results for adsorption and desorption, respectively (cumulative volume of adsorption and desorption, respectively).

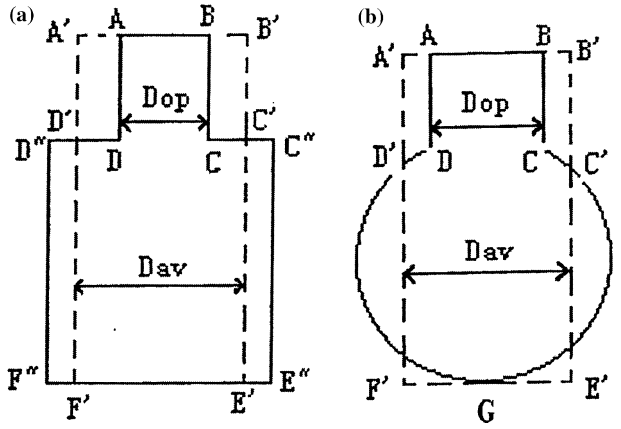

Figure 3. Shape of the cavity for adsorption of type IV and hysteresis loop of type E: (a) Wide "ink-bottle" shaped mesopores; (b) "Spheroidal cavities" (Type II ink-bottle) shaped mesopores.

Since, $V_{rl} = \pi\ (D_{av}{}^{op})^2/4 \times l$ and $V_l = \pi\ (D_{av}{}^{ads})^2/4 \times l$, we finally have:

$$(D_{av}^{op})^2/(D_{av}^{ads})^2 = V_{rl}/V_l \text{ or } (D_{av}^{op}) = (D_{av}^{ads}) \times (V_{rl}/V_l)^{1/2}$$

Thus, it is possible to calculate the diameter of the pore opening, $D_{av}{}^{op}$ or simply: D^{op} (calculted values reported in tables 1 and 2).

As expected, the controlled dealumination of the NaX and CaA zeolites led to almost amorphous and mesoporous materials (tables 1 and 2). The CaA gave much larger pore sized materials than the NaX because the treatment reaction with AHFS removed more Al species due to the higher Al content in the CaA zeolite. However, the (m) Na-deal X (calcined) showed narrower pore size distribution than the deal CaA (figure 4 and tables 1 and 2):

(m) Na-deal X (calcined): $d_{av} = 4.6 \pm 1.0$ nm;
deal-CaA (calcined): $d_{av} = 15.1 \pm 3.0$ nm

In addition, the value of the cumulative surface area (S_{cum}) obtained during the desorption phase of nitrogen in all our silica nanoboxes was much larger than the value of the BET surface area (tables 1 and 2): this might be ascribed to the existence of intersections between the capillaries [20b], i.e. our materials were not isolated but truly interconnecting nanoboxes.

3.2. Thermal stability of the new mesoporous materials

Calcination of the (m) Na-deal X sample resulted in some loss of surface area and sorption volume (table 1): this was due to some debris still trapped inside the mesoporous cavities upon AHFS treatment and which had agglomerated to larger internal particles due to the calcination, blocking thus some pores.

In terms of thermal stability, the calcined (m) H-deal X (final calcination temperature = 600°C), using the temperature-programmed (TPC) or direct heating (DH) procedures, still showed quite high surface areas and large sorption volumes (table 1). This was not predicted because normally the structure of the

Table 1
Nitrogen adsorption/desorption isotherms of the Na-X zeolite-derived mesoporous materials investigated in this work

Sample	BET (m^2/g)	S_{cum} (m^2/g)	S_{mic} (m^2/g)	Crystallinity (Si/Al)	D_{av} (nm)	D^{op} (nm)	V_t (cc/g)	V_{mes} (cc/g)	V_{mic} (cc/g)
NaX	740	–	696	High (1.2)	0.8	0.8	0.31	0.03	0.28
(m) Na-deal X (250°C)	451	509	0	Very low (1.7)*	4.6	4.0	0.54	0.53	0.00
(m) Na-deal X (600°C)	252	321	0	Amorphous*	4.7	4.0	0.38	0.37	0.00
(m) NH_4-deal X (250°C)	443	528	0	Amorphous*	4.7	4.1	0.57	0.52	0.00
(m) H-deal X (600°C, TPC)	328	419	0	Amorphous*	4.5	3.9	0.43	0.40	0.00
(m) H-deal X (600°C, DH)	281	399	0	Amorphous*	4.9	4.2	0.44	0.41	0.00
(b) Na-deal X (250°C)	363	282	133	n.a.	5.4	5.0	0.38	0.33	0.05
(b) NH_4-deal X (250°C)	234	252	45	n.a.	6.9	6.2	0.39	0.36	0.02
(b) H-deal X (600°C, DH)	8	8	0	n.a.	21.1	n.a.	0.04	0.04	0.00

*Except for peak of X-ray powder diffraction at low angles.
n.a. = not available.

Table 2
Nitrogen adsorption/desorption isotherms of the Ca-A zeolite-derived mesoporous materials investigated in this work

Sample	BET (m^2/g)	S_{cum} (m^2/g)	S_{mic} (m^2/g)	Crystallinity (Si/Al)	D_{av} (nm)	D^{op} (nm)	V_t (cc/g)	V_{mes} (cc/g)	V_{mic} (cc/g)
CaA	661	–	614	High (1.0)	0.5	0.5	0.27	0.02	0.25
Deal-CaA (250)	251	291	61	Very low (1.5)	15.1	14.5	0.80	0.77	0.03
Deal-CaA (600°C, TPC)	215	236	28	Amorphous	14.0	14.1	0.72	0.67	0.01

*Except for peak of X-ray powder diffraction at low angles.
n.a. = not available.

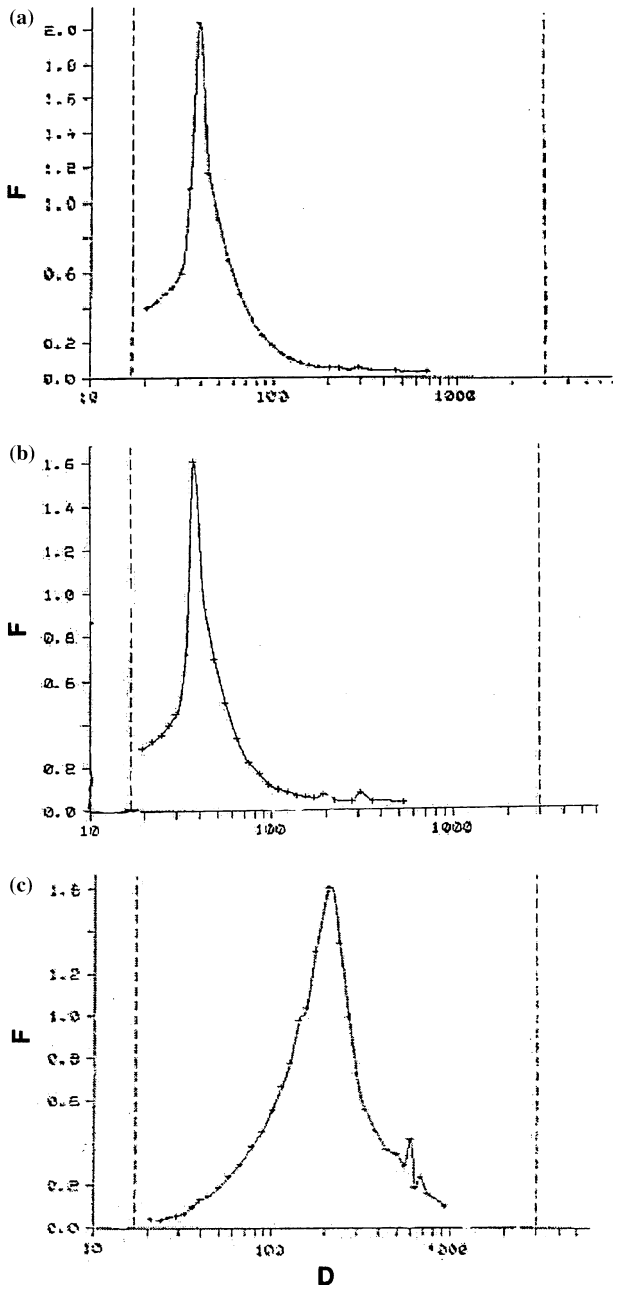

Figure 4. Pore size distribution curves ($F=[dV/d\log D]$) in $cm^3\ g^{-1}$ versus pore diameter D in 10^{-1} nm) of the new silica nanoboxes: (a) (m) Na-deal X (calcined at 600°C); (b) (m) H-deal X and (c) deal CaA (250°C).

ammonium form of the X zeolite starts to rapidly decompose at ca. 100°C [22]. The thermal stability of the (m) H-deal X might be due to its higher Si/Al ratio and its amorphous character. There was almost no change in terms of pore size distribution with respect to the (m) Na-deal X (figure 4). However, when the "bimodal" (b) NH_4-deal X sample was heated to 600°C, very low BET surface area and sorption volume were obtained (sample (b) H-deal X in table 1). Our first interpretation of these results is that when the (b) NH_4-deal X was heated rapidly to an elevated temperature, the sudden decomposition of ammonium ions into protons provoked the collapse of the remaining micropores, leading to the extraction of large Al containing debris with the obvious consequence of a significant pore blocking (occlusion). Such phenomena are currently under investigation using X-ray powder diffraction at low angles in combination with ^{29}Si and ^{27}Al solid-state NMR spectroscopy.

Therefore, to obtain highly thermally resistant silica nanoboxes, these materials should not contain any microporous (or less than 2–3%) remnant of the dealumination of the parent zeolite.

3.3. *Modification of the pore characteristics upon incorporation (and subsequent thermal treatment) of orthosilicate*

Orthosilicate (orthosilicic acid) species when incorporated into the ZSM5 zeolite which was subsequently activated at high temperature, could reduced the pore opening from an average of 0.55 to 0.47 nm [11]. The method when applied to our materials, particularly the (m) H-deal X, resulted in significant decreases in the pore opening (table 3). Unfortunately, the average pore diameter was also affected to almost the same extent. In addition, a maximum pore opening narrowing was observed with an incorporation of 20 wt% of orthosilicate, from 3.9 nm for the (m) H-dealX to 3.7 nm for the (20) H-deal X sample. Nevertheless, the incorporation of orthosilicate reinforces the walls of the silica nanoboxes and increases the number of hydroxyl groups which can be useful in various procedures of grafting of active functions.

Table 3
Modification of the pore characteristics upon incorporation of orthosilicate (and subsequent thermal treatment)

Sample	SiO_4 (wt%)	BET (m^2/g)	D_{av} (nm)	D^{op} (nm)	V_t (cc/g)	V_{mes} (cc/g)	V_{mic} (cc/g)	V_{mac} (cc/g)
(5) H-deal X	5	324	4.5	3.9	0.42	0.39	0.00	0.03
(10) H-deal X	10	343	4.4	3.9	0.44	0.40	0.00	0.04
(15) H-deal X	15	348	4.4	3.8	0.43	0.39	0.00	0.04
(20) H-deal X	20	347	4.4	3.7	0.42	0.38	0.00	0.04
(25) H-deal X	25	345	4.3	3.8	0.41	0.37	0.00	0.04
(40) H-deal X	40	331	4.2	3.8	0.38	0.34	0.00	0.04

Table 4
modification of the pore characteristics upon loading of sulfuric acid and triflic acid

Sample	Acid	Acid loading (wt%)	BET (m^2/g)	D_{av} (nm)	D^{op} (nm)	V_t (cc/g)	V_{mes} (cc/g)
(S15) H-deal X	H_2SO_4	15	252	4.9	4.1	0.35	0.32
(S20) H-deal X	H_2SO_4	20	236	4.9	4.1	0.32	0.30
(S25) H-deal X	H_2SO_4	25	151	5.5	4.4	0.25	0.24
(T7) H-deal X	Triflic ac.	7.2	327	4.6	4.0	0.44	0.41
(T10) H-deal X	Triflic ac.	10.0	282	4.6	3.7	0.39	0.36
(T16) H-deal X	Triflic ac.	15.6	244	4.6	3.9	0.36	0.33
(T24) H-deal X	Triflic ac.	23.6	215	4.7	3.9	0.31	0.29
(T32) H-deal X	Triflic ac.	32.0	101	5.2	4.2	0.18	0.17

3.4. *Chemical stability assessed by the maximum loading of sulfuric acid and triflic acid*

Incorporation of acidic species onto the surface of mesoporous materials may provide interesting acid catalysts with cavities sufficiently large to convert bulky molecules. Several techniques recently developed for the production of hydrothermally stable and strongly acidic mesoporous aluminosilicates include assemblies using protozeolitic seeds [23,24] and coating of protozeolitic nanoclusters onto the surface of preformed mesostructured aluminosilicates [3,25]. In our case, since our materials exhibited a network of cavities of an ink-bottle shape, it was our intention to incorporate – in quite significant amounts – liquid acidic species such as sulfuric acid (Hammett acidity function $H_o = -12.0$) and triflic acid, a superacid ($H_o = -14.1$) [13,26]) into these solid supports. The surface of these acidic systems could express catalytic properties as it were a free liquid surface, thus maybe in a more advantageous way than the simply supported catalysts in some reactions of industrial interest such as the isobutane/olefin alkylation [27] or others catalytic reactions [28]. In addition, at the end of the reaction, it would be possible to easily separate and recover the solid catalyst.

As expected, the mesoporous MCM-41 materials did not withstand any treatment with sulfuric acid or triflic acid since they underwent a total structural collapse. This was not the case for our mesoporous sample (m) H-deal X which allowed a loading of sulfuric acid up to 20 wt% and triflic acid up to 16 wt% while giving quite decent surface areas and pore volumes (table 4). This meant that the walls of the (m) H-deal X were not merely a quite fragile stacking of silica layers such as in the MCM-41 materials, but their structure was actually similar to that of the walls of siliceous zeolites. As shown in figure 5, by using the DTA/TGA technique, it was possible to qualitatively assess the amounts of triflic acid in the liquid and the bound phases, respectively. In fact, with the (T24) H-deal X (24 wt% of triflic acid originally loaded), there was desorption (see the sign of the corresponding DTA peak, figure 5b) at 200–220°C of some sorbed species (more than 4 wt%) which could be easily attributed to the free triflic acid form (boiling point = 161°C [26]). At 280–340°C, there was instead decomposition (see the sign of the corresponding DTA peak) of other surface species (more than 15 wt%) which were assigned to the bound triflic acid [16]. On the

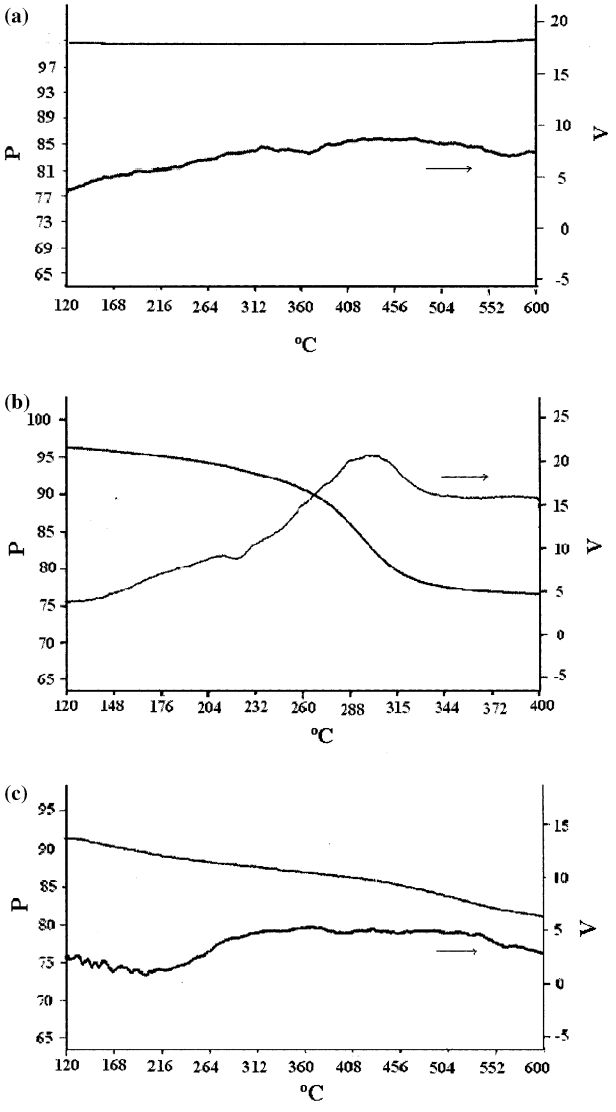

Figure 5. DTA/TGA analyses [*P*(%) and V(microvolts); argon] performed on the following samples: (a) parent (m) H-deal X; (T24) H-deal X; and (c) (S20) H-deal X.

other hand, the material loaded with sulfuric acid did not show such clear distinction between surface species (figure 5c) because sulfuric acid reacted readily with Al atoms which were gradually removed from their locations as the temperature increased.

Finally, the conditions for obtaining monomodal silica nanoboxes by dealumination of NaX or CaA were as follows:

– absence of microporosity
– significantly high surface area and pore volume
– narrow mesopore size distribution

4. Conclusion

In recent years, several nanomaterials expected to have interesting applications in catalysis, separation technology and chemical sensing have been synthesized [1–3,23–25,29]. In particular, in some catalytic applications, strong surface acidity and high thermal stability are essential [3,24]. In this work, we report the production of new thermally (using both the TPC and DH procedures of calcination) and chemically stable nanomaterials having periodic arrangement of interconnecting mesopores. These (monomodal) silica nanoboxes whose network is constituted of solely mesopores and which are prepared by controlled dealumination of alumina-rich zeolites, have pore characteristics which depend on the parent zeolites: the alumina-richer the zeolite, the narrower the mesopores of the resulting nanoboxes. The new materials can host strong acidic species to a significant amount.

Prospects for applications of the new silica nanoboxes are particularly brilliant in Catalysis (encapsulation of ''liquid'' acidic species and ionic liquids, the latter might be used as media for organic synthesis [30]) and in Separation technology (for instance, separation of proteins by gel-filtration chromatography or by ultrafiltration using pinholes-free membranes or filters prepared by special techniques [31]).

Acknowledgments

The authors thank the Natural Sciences and Engineering Research Council of Canada (NSERC) for financial support. Technical assistance from Mrs. A. Urbanska, Dr. G. Denes, Dr. J.P. Chartrand (CANMET-Ottawa) and Q. Zhao is acknowledged.

References

[1] C.T. Kresge, M.E. Leonowicz, W.J. Roth, J.C. Vartuli and J.S. Beck, Nature 359 (1992) 710.
[2] J.S. Beck, J.C. Vartuli, W.J. Roth, M.E. Leonowicz, C.T. Kresge, K.D. Schmitt, X.T.-W. Chu, D.H. Olsen, E.W. Sheppard, S.B. Sheppard, S.B. McCullen, J.B. Higgins and J.L. Schlenker, J. Am. Chem. Soc. 114 (1992) 10834.
[3] T.-O. Do and S. Kaliaguine, Angew. Chem. Int. Ed. 40(17) (2001) 3248 and references therein.
[4] R. Le Van Mao, N.T.C. Vo, B. Sjiariel, L. Lee and G. Denes, J. Mater. Chem. 2(6) (1992) 595.
[5] R. Le Van Mao, N.T.C. Vo, G. Denes and T.S. Le, J. Porous Mater. 1 (1995) 175.
[6] R. Le Van Mao, J.A. Lavigne, B. Sjiariel and C.H. Langford, J. Mater. Chem. 3(6) (1993) 679.
[7] R. Le Van Mao, G. Denes, N.T.C. Vo, J.A. Lavigne and S.T. Le, Mat. Res. Soc. Symp. Proc. 371 (1995) 123.
[8] C. Marcilly, in: *Catatyse Acido-basique: Application au raffinage et a la petrochimie*, Vol. 2 (ed.), (Technip, Paris, 2003), p. 720 and refs therein.
[9] A.H. Janssen, A.J. Koster and K.P. de Jong, Angew. Chem. Int. Ed. 40(6) (2001) 1102.
[10] G.W. Skeel and D.W. Breck, in: *Proc. 6th Int. Zeolite Conf., Reno (U.S.A.)*, eds. D. Olson and A. Bisio (Butterworths, Guilford, 1984), p. 87.
[11] D. Ohayon, R. Le Van Mao, D. Ciaravino, H. Hazel, A. Cochennec and N. Rolland, Appl. Catal. A: General 217 (2001) 241.
[12] Q.L. Wang, G. Giannetto and M. Guisnet, Zeolites 10 (1990) 301.
[13] P.J. Stang and M.R. White, Aldrichim. Acta 16(1) (1983) 15.
[14] E.P. Barrett, L.G. Joyner and P.P. Halenda, J. Am. Chem. Soc. 73 (1951) 373.
[15] K.S.W. Sing, D.H. Everett, R.A.W. Haul, L. Moscou, R.A. Pierotti, J. Rouquerol and T. Siemienewska, Pure Appl. Chem. 57 (1985) 603.
[16] R. Le Van Mao and L. Huang, in: *Novel Production Methods for Ethylene, Light Hydrocarbons, and Aromatics*, eds. L.F. Albright, B.L. Crynes and S. Nowak (Marcel Dekker, New York, 1992), p. 425.
[17] R.B. Borade and A. Clearfied, Catal. Lett. 31 (1995) 267.
[18] J. Fripiat, J. Chausson and A. Jelli, *Chimie-Physique des Phenomenes de Surface* (Masson et Cie, Paris, 1971) 26.
[19] A.J. Lecloux, in: *Catalysis Science and Technology*, Vol. 2 J.R. Anderson and M. Boudart eds., (Springer-Verlag, Berlin, 1981), p. 171.
[20] (a) J.H. de Boer, in: *The Structure and Properties of Porous Materials*, eds. D.H. Everett and F.S. Stone (Butterworths, London, 1958), p. 68; (b) J.H. de Boer, ibidem, p. 88.
[21] M. Suzuki, *Adsorption Engineering* (Kodansha-Elsevier, Tokyo, 1990) 26.
[22] D.W. Breck, *Zeolite Molecular Sieves* (J. Wiley & Sons, New York, 1974) 495.
[23] Y. Liu, W. Zhang and T.J. Pinnavaia, J. Am. Chem. Soc. 122 (2000) 8791.
[24] Y. Liu and Y.J. Pinnavaia, J. Mater. Chem. 12 (2002) 3179.
[25] T.-O. Do, A. Nossov, M.-A. Springuel-Huet, C. Schneider, J.L. Bretherton, C.A. Fyfe and S. Kaliaguine, J. Am. Chem. Soc. 126 (2004) 14324.
[26] G.A. Olah, G.K. Sueya Prakash and J. Sommer, *Superacids* (J. Wiley & Sons, New York, 1985) 36–37.
[27] J.F. Joly, in: *Conversion Processes*, Vol. 3 P. Leprince (ed.), (Editions Technip, Paris, 2001), pp. 287–288.
[28] R. Le Van Mao and T.S. Le, in: *Handbook of MTBE and Other Gasoline Oxygenates*, eds. H. Hamid and M.A. Ali (Marcel Dekker, New York, 2004), p. 93.
[29] K. Landskron and G.A. Ozin, Science 306 ((26 Nov. 2004)) 1529.
[30] C & EN, (Nov. 8, 2004), p. 44.
[31] R. Le Van Mao, E. Rutinduka, C. Detellier, P. Gougay, V. Hascoet, S. Tavakoliyan, S.V. Hoa and T. Matsuura, J. Mater. Chem. 9(3) (1999) 783.